Quantum Field Theory of Inelastic Diffraction.
IV. Applications to Al(100) and Al(111)[*]

C. B. Duke[†] and U. Landman[†]

*Department of Physics, Materials Research Laboratory, and Coordinated Science Laboratory,
University of Illinois, Urbana, Illinois 61801*

(Received 27 March 1972)

Results are presented of numerical calculations of the inelastic-low-energy-electron-diffraction (ILEED) intensities of electrons inelastically scattered into the (00) beam from Al(100) and Al(111) via the emission of bulk and surface plasmons. The calculations are based on the isotropic-scatterer version of the theory described in Paper III of this series. The results ex-exhibit three important systematic features. First, dynamical effects (i.e., those not evident in a kinematical two-step model) are prominent in plots of diffracted intensity versus incident-beam energy (energy profiles), smaller in plots of these intensities versus the electron's exit angle (angular profiles), and unimportant in plots of scattered intensities versus energy loss (loss profiles). Second, dynamical effects in the energy profiles are readily discernible even for weak electron–ion-core scattering. Finally, the contributions to the diffracted intensities due to the "three-step" diffraction-before-and-after-loss processes are found to be exceedingly small relative to those associated with the "two-step" processes of diffraction before or after loss. These features permit us to draw two important conclusions from our analysis. First, the extraction from experimental ILEED intensities of surface-plasmon dispersion relations may be based on a kinematical two-step model provided the analysis is confined to a consideration of loss and angular profiles. Second, the consequences of the vestiges of momentum conservation normal to the surface in a kinematical-model calculation of the excitation of bulk plasmons cannot be distinguished clearly from those of multiple elastic scattering. Thus kinematical momentum-conservation conditions for motion normal to the surface seem to be entirely irrelevant in the interpretation of ILEED intensities.

I. INTRODUCTION

In this paper we present the results of numerical calculations of inelastic-low-energy-electron diffraction (ILEED) intensities based on the theory developed in the preceding paper[1] (Paper III in the series [1–3]). Our primary objective is not the evaluation of the cross sections *per se*, but the extraction from the model predictions of general features of the dynamical theory of ILEED, analogous to our previous studies[4–6] of elastic low-energy-electron diffraction (ELEED) based on the same type of model. To this end, we present sample results for surfaces with the geometries of Al (100) and Al (111) by way of illustration of the consequences of our dynamical theory.[1]

In the analysis presented in the preceding paper, we evaluated the scattering cross sections of electrons which are inelastically reflected from a single-crystal solid surface after having excited a single bulk or surface plasmon. We summed all perturbation-theory contributions to these cross sections in which the incident electron scattered elastically from the ion cores in the solid an arbitrary number of times but interacted only once with a plasmon. This analysis revealed that the consideration of multiple-elastic-scattering processes led to two main consequences relative to the earlier[3] kinematical model of two-step inelastic diffraction. First, for those classes of perturbation-theory diagrams in which all of the multiple-elastic-scattering events occur before (after) the loss, the summation over these events leads simply to the renormalization of the elastic electron–ion-core scattering vertices. In these cases the earlier interpretation[3] of inelastic diffraction in terms of two-step "diffraction-before-loss" ("loss-before-diffraction") processes remains intact. The second consequence of multiple elastic scattering, however, is the occurrence of diagrams describing elastic events both before and after the loss. When summed, these diagrams lead to "three-step" processes, in which a renormalized elastic-scattering vertex occurs both before and after the loss vertex.

Given these analytical results, in this paper we focus our attention on three central issues. First, how large are the three-step relative to the renormalized two-step contributions to the ILEED intensities? Second, what is the general order of magnitude of explicitly dynamical (i.e., multiple-scattering) phenomena in the predicted inelastic cross sections? Third, given the dynamical nature of ILEED as well as ELEED, how accurately must the effective electron-solid force law for elastic electron-solid scattering be known in order to use the theory to extract from observed ILEED intensities the dispersion and damping of the plasmons

excited by the inelastically scattered electrons?

Within the context of our calculations (which are based on the isotropic-scatterer model[1-6] of the elastic electron–ion-core scattering) the first issue is resolved simply: the three-step contributions to the ILEED intensities usually are an order of magnitude smaller than the two-step contributions. However, a major outcome of our examination of the second two questions is the discovery that the answers to them depend on the selection of the fashion in which the inelastic-diffraction intensities are displayed. Any mode of presentation in which the beam parameters of the elastic-scattering vertices sweep over wide ranges (i.e., $\Delta E \gtrsim 25$ eV, $\Delta\theta$, $\Delta\psi \gtrsim 10°$) is accompanied by the prominent appearance in the predicted intensities of dynamical effects and, occasionally, by the importance of three-step diffraction processes. Consequently, specifically dynamical features of the predicted ILEED intensities are most easily discerned in plots of the scattered intensity versus incident electron energy (E) for fixed incident polar (θ) and azimuthal (ψ) angles, fixed polar (θ') and azimuthal ($\psi' \equiv \psi + \pi$) exit angles, and fixed electron energy loss ($w = E' - E$). Following the nomenclature of Laramore and Duke[3] we call such curves "energy profiles." It also is convenient to present the inelastic cross sections as "angular profiles" defined to be plots of the scattered intensity versus exit angle (θ') for fixed incident-beam parameters (E, θ, ψ) and exit-beam azimuth and energy loss ($\psi' = \psi + \pi$, w). In such angular profiles, the multiple scattering exerts little influence on maxima associated with surface plasmons, but considerable influence on those associated with bulk plasmons. In particular, the manifestations of the phenomenon of sideband diffraction,[3,7,8] caused by the vestiges in a kinematical model of momentum conservation normal to the surface for energy loss to bulk plasmons, cannot be distinguished clearly from those of multiple elastic scattering.

A presentation of the inelastic cross sections in which the consequences of multiple scattering are almost negligible (except for a constant scale factor) is the "loss profile" in which the intensities are displayed as functions of the electron energy loss (w) for constant incident-beam parameters (E, θ, ψ) and constant exit-beam angles (θ', ψ'). These loss profiles reflect directly the spectral density[1,2] associated with both the surface- and bulk-loss processes. Therefore, by analyzing them for various values of loss energy and exit angle, the dispersion and damping of the excitations created by the electron can be determined.[9-11] If multiple-scattering effects influenced these loss profiles in an important way, then it would be necessary to have a good theoretical description of the observed ELEED intensities as a precondition to

determining the dispersion and damping of the excitations created by the electrons undergoing ILEED. Our verification that the loss profiles are insensitive to dynamical multiple-scattering effects indicates that a reliable determination of excitation dispersion and damping can be performed even if the elastic electron-solid interaction is not known precisely (i.e., a detailed description of the observed ELEED intensities has not been achieved). In addition the data analysis can be carried out using a simple kinematical two-step model rather than a more complicated (and computer-time consuming) dynamical model. As the electron-solid interactions are not known with high accuracy for low-energy ($10 \lesssim E \lesssim 500$ eV) electrons,[12-14] these conclusions are critically important for the justification of the use of ILEED as a spectroscopic probe of the excitation spectra of solids.

We proceed by first reviewing in Sec. II the definition of the parameters which are used in the model calculation. Because of the dependence on the mode of presentation of the nature of the interpretation of the intensities, we organize the remainder of the paper by presenting, in turn, sample calculations for the inelastic energy (Sec. III), angular (Sec. IV), and loss (Sec. V) profiles. Our discussion of the energy profiles centers around the identification of the magnitude of dynamical effects in the inelastic-diffraction intensities. Our treatment of the angular and loss profiles emphasizes the more minor nature of the dynamical effects evident in these methods of displaying the intensities, and their resulting use in determining surface-plasmon dispersion relations. Finally, we give in Sec. VI a summary of our results and the conclusions we have drawn from them. All technical details of the calculations have been omitted because they are given in papers I-III of this series.[1-3] Therefore, this paper provides a self-contained survey, within the framework of the isotropic-scatterer model of elastic electron–ion-core scattering, of the physical consequences of our theory for those readers who are not interested in its mathematical structure.

II. DEFINITION OF MODEL PARAMETERS

The model Hamiltonian used in the calculation of the ILEED intensities presented herein is described in Sec. II of the preceding paper,[1] For convenience, in this section we review the definitions of the parameters which characterize this model and, consequently, which must be specified in order to make the results shown in the figures well defined.

The elastic scattering of the electron from the ion cores in the solid is given in terms of at most four parameters. The consequences of the electron-electron interactions are described by the real part of the one-electron proper self-energy

("inner potential") V_0 and the inelastic-collision damping length λ_{ee}. These are related to the one-electron proper self-energy via Eqs. (14) in the preceding paper[1] as originally described and justified by Duke et al.[2,15,16] The electron-lattice interactions are specified within the isotropic-scatterer model[4,16] by the s-wave phase shift δ_s associated with the planar surface layer of scatterers, and that, δ_B, associated with "bulk" scatterers. Often we take the surface and bulk scatterers to be identical, i.e.,

$$\delta_S = \delta_B = \delta \ . \tag{1}$$

Calculations of the inelastic-scattering cross sections require that we specify the plasmon-dispersion relations as well as elastic and inelastic electron-solid interaction vertices. The latter are given in Sec. II of the preceding paper.[1] To obtain the former, we follow Bagchi and Duke.[9,10] The bulk-plasmon dispersion is given by

$$\hbar\omega_b(p) = 14.2 + 3.048p^2 \ , \tag{2a}$$

$$\Gamma_b(p) = 0.53 + 0.103p^2 + 1.052p^4 \ . \tag{2b}$$

Energies are measured in electron volts and momenta in reciprocal angstroms. Except for the threshold value of 14.2, all of the parameters are obtained from kilo-electron-volt thin-film transmission experiments as described by Bagchi and Duke. For the surface-plasmon dispersion we use Bagchi and Duke's "best-fit" values obtained by analyzing experimental data on Al (111):

$$\hbar\omega_s(p_\shortparallel) = 10.1 - 0.7p_\shortparallel + 10p_\shortparallel^2 \ , \tag{3a}$$

$$\Gamma_s(p_\shortparallel) = 0.9 + 0.76p_\shortparallel \ . \tag{3b}$$

Subsequent analyses[17] have shown other dispersion relations to be in equally good agreement with more extensive data,[18] although corrections to a normalization constant in Bagchi and Duke's computer program[9] lead to a larger value of $\Gamma_s(0)$ [i.e., $\Gamma_s(0) \simeq 1.4$ eV rather than 0.9 eV]. However, both of these refinements of the data analysis are neglected here so that our figures labeled "kinematical" are directly comparable to those presented by Bagchi and Duke. The combination of the four elastic-scattering parameters V_0, λ_{ee}, δ_S, and δ_B, the inelastic electron-plasmon vertices specified in Eqs. (5) and (10) in Duke and Landman,[1] and the dispersion relations given by Eqs. (2) and (3), suffices to define uniquely the calculation of the ILEED intensities using the formulas presented in Sec. IV of the preceding paper. The results of such calculations are displayed and discussed in Secs. III-V.

III. ENERGY PROFILES: Al (100)

To examine the dynamical effects evident in the predicted inelastic-diffraction intensities, we pres-

ent sample calculations of energy profiles of the (00) beam of electrons scattered from Al (100) at an incident polar angle of $\theta = 15°$, and azimuthal plane containing a unit vector of the primitive surface unit cell. For reference, we present in Fig. 1 the elastic ($w = 0$) energy profiles for several different models of the electron–ion-core interactions. In the case of "weak" elastic scattering, i.e., $\delta = \frac{1}{10}\pi$, the kinematical primary Bragg
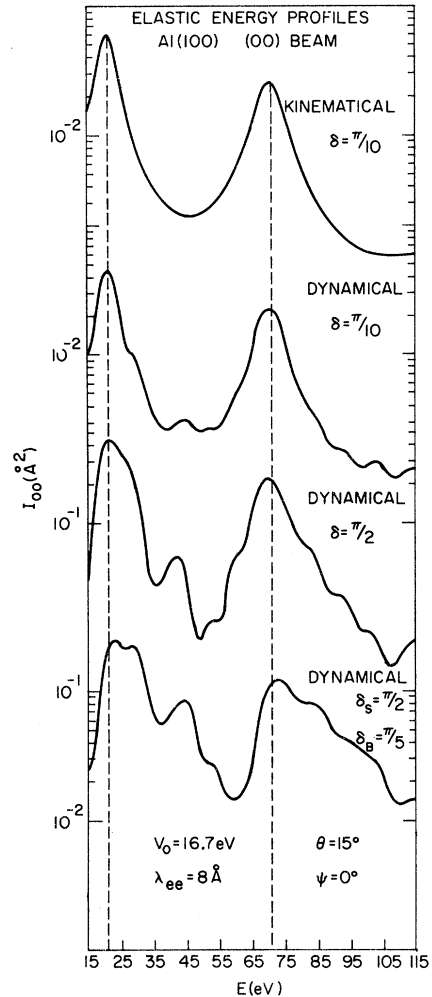

FIG. 1. Elastic energy profiles for the (00) beam of electrons scattered from Al(100). The primary and final polar angles of incidence and exit, respectively, are 15°. Both incident and exit beams lie in a plane containing a unit vector of the primitive unit surface cell. The dynamical elastic-scattering parameters are indicated in the figure. All "dynamical" calculations were performed for a rigid-lattice model using the isotropic-scatterer, inelastic-collision-model analysis of Tucker and Duke (Ref. 4). The "kinematical" calculations are performed using the Born approximation. Vertical dashed lines designate the energies of the kinematical primary Bragg peaks.
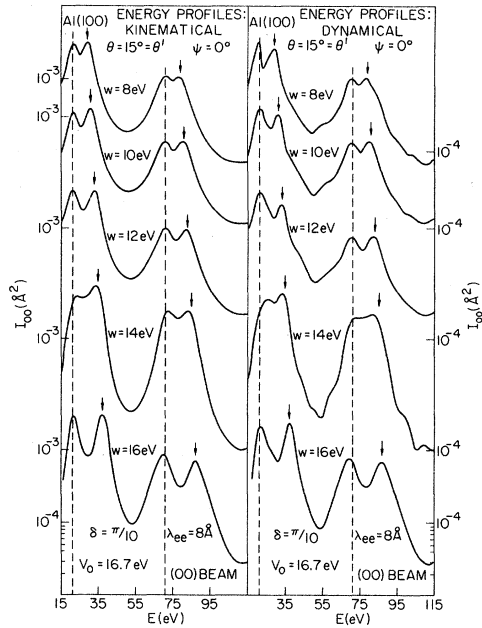
FIG. 2. The kinematical (left-hand panel) and dynamical (right-hand panel) inelastic energy profiles for the (00) beam of electrons diffracted from Al(100). The beam parameters and the parameters used to describe the elastic-electron-solid scattering are indicated in the figure. Vertical dashed lines indicate the energies E_B of the kinematical Bragg peaks in the elastic energy profiles. Downward-pointing arrows designate the energies $E_B + w$. The "kinematical" profiles were evaluated using the two-step model of Bagchi and Duke (Refs. 9 and 10). The "dynamical" profiles were evaluated according to Eqs. (23)–(41) in Duke and Landman (Ref. 1). The plasmon-dispersion relations were taken to be those of Bagchi and Duke (Ref. 9): $\hbar\omega_s(p_\parallel) = 10.1 - 0.7p_\parallel + 10p_\parallel^2$; $\Gamma_s(p_\parallel) = 0.9 + 0.74p_\parallel$, $\hbar\omega_b(p) = 14.2 + 3.048p^2$; and $\Gamma_b(p) = 0.53 + 0.103p^2 + 1.052p^4$. All energies are measured in electron volts and momenta in reciprocal angstroms.

peaks occurring at energies of 21 and 71 eV persist when going from the kinematical to the dynamical description. However, a secondary peak at 45 eV, missing in the kinematical curve, occurs in the dynamical results. Additional dynamical structure also is evident for energies $E > 75$ eV. The dynamical structure is enhanced by going to a stronger electron–ion-core scattering ($\delta = \frac{1}{2}\pi$) for a truncated bulk solid or enhanced scattering of the surface (δ_s) relative to the bulk (δ_B) ion cores. All of the calculations are performed using the rigid-ion, isotropic scatterer model of Tucker and Duke.[4] The results for a relatively large ($\lambda_{ee} = 8$Å) inelastic-collision damping length are presented in order to illustrate the dynamical effects evident in the cross sections.

In Fig. 2 we present the kinematical and dynamical inelastic energy profiles in the weak-scattering limit for a series of loss energies (w). In this

limit, the diffraction before loss (D-L) and the loss followed by diffraction (L-D) peaks occur (as expected[1,3]) at the same energies in both of the calculated intensities. However, dynamical effects are evident in the predicted line shapes, especially for those values (10 and 14 eV) of the loss energy near the surface- and bulk-plasmon excitation thresholds (10.1 and 14.2 eV, respectively).

The dynamical effects become more prominent for larger values of the electron–ion-core elastic scattering phase shift as shown by Fig. 3 in which we compare results for the dynamical theory in the case of weak and strong elastic scattering from a truncated "bulk" solid. A three-or-four maximum structure is observed in the strong-scattering case for $15 \lesssim E \lesssim 45$ eV. The kinematical two-step model predicts only two maxima in this energy range (see Fig. 2). Thus, we see that in the inelastic energy profiles, multiple-scattering phenomena can cause the same splitting of the inelastic doublet structure as the sideband-diffraction phenomenon.[7,8] This phenomenon consists of the prediction of extra maxima when the kinematical-momentum-conservation condition associated with the excitation of a
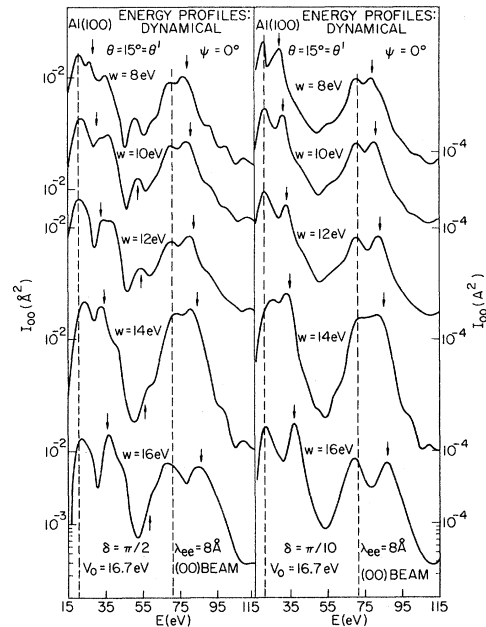

FIG. 3. Comparison between the weak-scattering ($\delta = \frac{1}{10}\pi$) and strong-scattering ($\delta = \frac{1}{2}\pi$) dynamical inelastic energy profiles for the (00) beam of electrons scattered from Al(100). Dashed lines indicate the energies of the kinematical primary Bragg peaks. The downward-pointing arrows indicate the energies $E_i \equiv E_B + w$ whereas the upward-pointing arrows designate dynamical secondary peaks. The elastic scattering parameters are indicated in the figure. The plasmon-dispersion relations used in the calculation, via Eqs. (23)–(41) in Duke and Landman (Ref. 1), are given in the caption to Fig. 2.
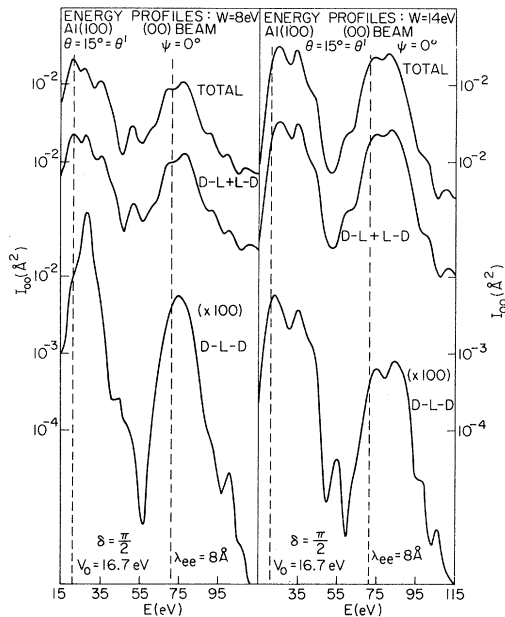
FIG. 4. Various contributions to the dynamical inelastic energy profiles at loss energies $w = 8$ and 14 eV for the (00) beam of electrons scattered from Al(100). The upper curves designate the cross section obtained by taking into account diffraction before loss (D-L), loss before diffraction (L-D), and diffraction before and after loss (D-L-D) as defined in Eqs. (20)−(23) in Duke and Landman (Ref. 1). The center curves give the renormalized two-step contribution (D-L and L-D) to the cross sections. The lower curves describe the three-step contributions (D-L-D) alone. Vertical dashed lines indicate the energies of prominent maxima in the elastic intensity profiles (see Fig. 1). The plasmon-dispersion relations used in the analysis are indicated in the caption to Fig. 2.

bulk-loss mode normal to the surface is satisfied at incident-beam energies which differ from the kinematical Bragg energies by more than the intrinsic width of the peaks in the energy profile. In our model, sideband-diffraction maxima are associated with bulk plasmons of large energy (i.e., momentum normal to the surface). Figure 2 indicates that they do not occur for this particular numerical example, although Fig. 3 clearly reveals a dynamical splitting of the doublet energy profiles for $w = 16$ eV which could have been misinterpreted as indicating sideband diffraction. However, this dynamical fine structure also occurs for $w < \hbar\omega_b(0)$ in which case sideband diffraction is impossible.

Having demonstrated the importance of considering dynamical effects in the interpretation of the energy profiles, let us examine the origin of these effects. Two types of questions immediately arise: What is the relative importance of surface- and bulk-plasmon excitations in causing a given "observed" structure? How large are the contribu-

tions of the three mechanisms [diffraction before loss (D-L); loss before diffraction (L-D), and diffraction before and after loss (D-L-D)] of inelastic diffraction?

Turning first to the latter question, the contributions to the inelastic cross sections from a renormalized two-step mechanism are compared to the contributions arising from the three-step processes in Fig. 4. It is evident that the contribution of the three-step process is nearly negligible for both values of w. Consequently, we identify the dynamical structures with the renormalization of the elastic-scattering vertices in the "two-step" mechanism.

We still must examine the magnitudes of the D-L and L-D mechanisms as well as the relative significance of bulk- and surface-plasmon losses for a given value of the loss energy w. To do this, we consider the case of enhanced elastic scattering from the surface layer ($\delta_S > \delta_B$) in order to accentuate the dynamical fine structure in the energy profiles (see, e.g., Fig. 1). Typical inelastic energy profiles for this case are shown in Fig. 5 in which the separate D-L and L-D as well as surface- and bulk-plasmon contributions also are displayed explicitly. Comparison of the contributions of the D-L and L-D mechanisms with the complete profile (top panel, Fig. 5) illustrates the persistence in the total scattered intensity of fine structure associated with the L-D process. The total intensity is not a simple sum of the L-D and D-L intensities because these two processes are coherent (i.e., they lead to the same final state). However, the surface- and bulk-plasmon contributions (lower two panels in Fig. 5) do add to give the total intensity because they are incoherent. As expected, for $w \lesssim 12$ eV the surface-plasmon-emission contribution dominates that associated with bulk-plasmon emission. Note, however, the substantial importance of the surface-plasmon process even at $w = 14$ eV for $40 \lesssim E \lesssim 60$ eV. Also, the surface-plasmon contribution to the intensity exhibits considerably more dynamical fine structure than that of the bulk plasmons because of the absence of the integration over components of momenta normal to the surface.

IV. ANGULAR PROFILES: Al (111)

The central issue in our study of angular profiles is whether or not prominent peaks in these profiles can be identified with surface plasmons in accordance with the kinematical two-step model as used by Bagchi and Duke[9] to determine the surface-plasmon-dispersion relation. A secondary but important question concerns the effects of multiple scattering on the line shapes themselves. In particular, does the large-angle peak of the surface-plasmon doublet disappear at incident electron energies approximately equal to a surface-plas-
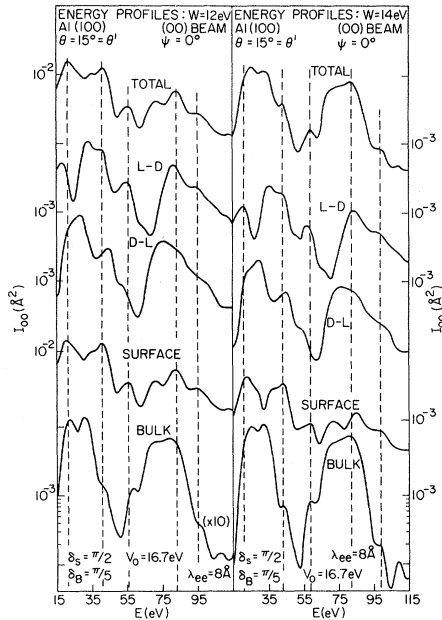
FIG. 5. Various contributions to the dynamical inelastic energy profiles for the (00) beam of electrons scattered from Al(100), for loss energies $w = 12$ and 14 eV. The beam parameters and those used to describe the elastic electron-solid diffraction are indicated in the figure. The plasmon-dispersion relations used in the analysis are given in the caption to Fig. 2. The labels L-D and D-L designate the loss-before-diffraction and diffraction-before-loss contributions to the cross section, respectively, as specified by Eqs. (28), (30), (31), and (36)–(38) in Duke and Landman (Ref. 1). The labels "surface" and "bulk" indicate the calculated intensities using only surface- and bulk-plasmon emission, respectively. Vertical dashed lines are solely to guide the eye to identify the energies of prominent structures in the intensities (see also Fig. 1).

model and the kinematical "two-step" model would give the same surface-plasmon-dispersion relation. More generally, we see that the "three-step" D-L-D contribution to the angular profile is negligible in the dynamical model, leading to a simple "two-step" interpretation in this as well as the kinematical model. The two incident-beam-energies $E = 50$ and 60 eV, were chosen to be the energy of a Bragg peak in the kinematical energy
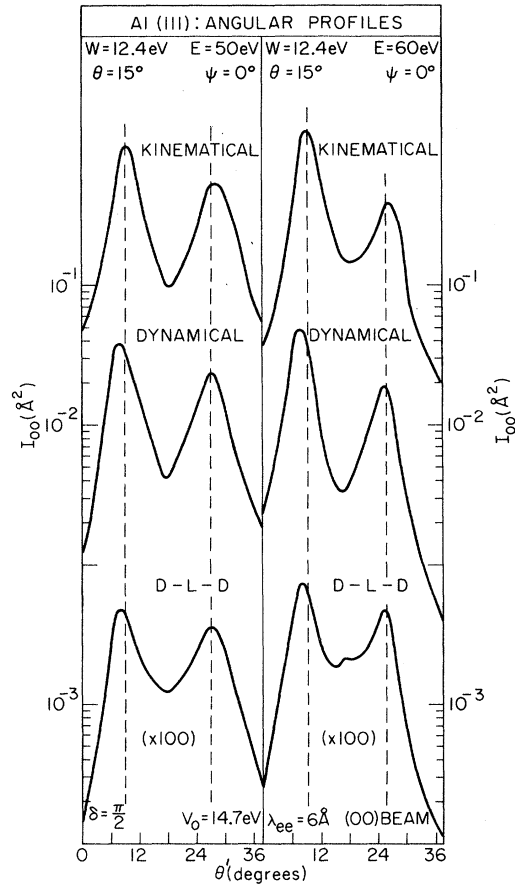

FIG. 6. Kinematical and dynamical angular profiles for electrons diffracted in the (00) beam from Al(111), for primary-beam energies of 50 eV (left-hand panel) and 60 eV (right-hand panel). The above energies correspond to those of a prominent peak in the kinematical elastic energy profile and to a surface-plasmon energy above the aforementioned peak energy, respectively (see e.g., Fig. 8). The loss of $w = 12.4$ eV (above the threshold for surface-plasmon excitation but below the one corresponding to bulk-plasmon excitation) is the one analyzed by Bagchi and Duke (Ref. 9). We also use Bagchi and Duke's dispersion relations for the bulk and surface plasmons (see caption to Fig. 2). The notation D-L-D designates the contribution from diffraction before and after loss as defined in Eq. (22) in Duke and Landman (Ref. 1). The parameters used in the model of the elastic-scattering cross section are noted in the figure. Vertical dashed lines are included for convenience in visualization.

mon energy above a prominent ("Bragg") peak in the elastic energy profile [see, e.g., Fig. 1 for Al (100)] as is the case experimentally?

Both of these questions are resolved by a comparison of the "dynamical" and "kinematical" angular profiles shown in Figs. 6 and 7 for loss energies w of 12.4 and 14.4 eV, respectively. At $w = 12.4$ eV only surface-plasmon emission is important, as is evident by the simple doublet structure in the angular profiles associated with the exit momenta:

$$\vec{k}_{\parallel}' = \vec{k}_{\parallel} \pm \vec{p}_{\parallel}(w) \; , \tag{4a}$$

$$w = \hbar\omega_s(\vec{p}_{\parallel}(w)) \; . \tag{4b}$$

Despite a tendency for the low-angle maximum to occur a degree or so sooner in the dynamical than in the kinematical profile, we see that for the purpose of rough data analysis,[9,17] the dynamical
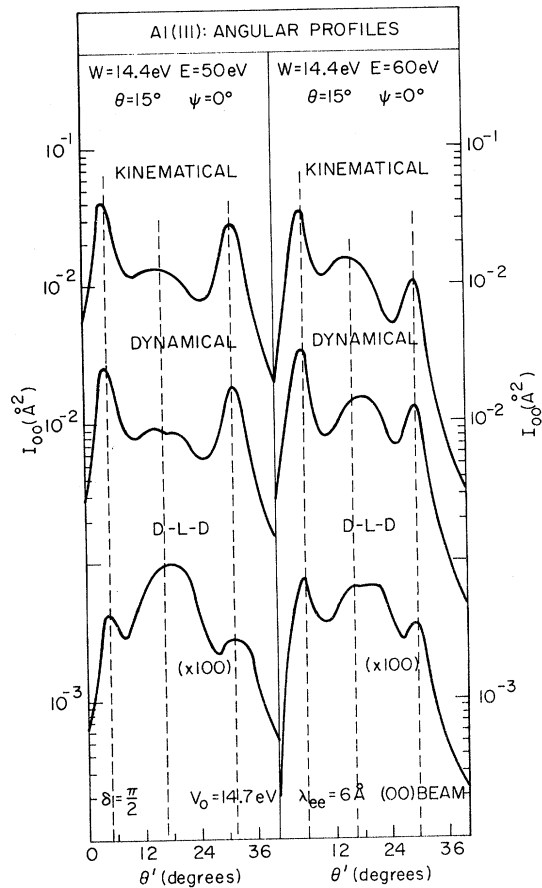
FIG. 7. Kinematical and dynamical angular profiles
for electrons diffracted in the (00) beam from Al(111),
for primary-beam energies of 50 eV (left-hand panel)
and 60 eV (right-hand panel). These energies correspond
to those of a prominent peak in the kinematical elastic
energy profile ($E = 50$ eV) and to a surface-plasmon's
energy above the aforementioned peak energy, respectively
($E = 60$ eV; see also Fig. 8). The loss energy of $w = 14.4$
(above the thresholds for both surface- and bulk-plasmon
excitation) is the one analyzed by Bagchi and Duke (Ref.
9). We also use Bagchi and Duke's dispersion relations
for bulk and surface plasmons (see caption to Fig. 2).
The notation D-L-D designates the contribution from dif-
fraction before and after loss as defined in Eq. (22) in
Duke and Landman (Ref. 1). The parameters used in the
model of the elastic-scattering cross section are noted in
the figure. Vertical dashed lines are included for con-
venience in visualization.

profile [see, e.g., Fig. 8(b)] and that of this Bragg
peak plus a surface-plasmon energy. Therefore
the D-L process dominates the profiles at $E = 50$
eV, whereas the L-D process is the largest at
$E = 60$ eV. Evidently the similarity between the
surface-plasmon peaks in the kinematic and dynam-
ical profiles persists in both cases.

The angular profiles for a loss energy ($w = 14.4$
eV) just above the bulk-plasmon threshold energy

[$\hbar\omega_b(0) = 14.2$ eV] are shown in Fig. 7. The cor-
respondence between the surface-plasmon peaks
($\theta' \sim 5°$, 30°) in the kinematical and dynamical pro-
files persists in this case also. However, dynam-
ical fine structure occurs in the bulk-plasmon peak
near $\theta' = 17°$. At $E = 50$ eV this peak is split into a
doublet whereas at $E = 60$ eV it is shifted by about
3° to 4° relative to the kinematic peak. Therefore,
we see that in the angular as well as energy pro-
files, the manifestations of sideband diffraction
cannot be separated unambiguously from those of
multiple-scattering effects.

Finally, we note that although the large-angle
peak in the surface-plasmon doublet is substantial-
ly lower in intensity at $E = 60$ eV than at $E = 50$ eV
(for both values of w), it is not completely obliter-
ated as suggested by available experimental
data.[9,11,18] This conclusion holds for both the
kinematical and dynamical models. Thus multiple-
scattering effects do not resolve this discrepancy
between the kinematical model and the available
data. It is possible that this result is a conse-
quence of our use of perturbation theory to de-
scribe the inelastic electron-solid interaction ver-
tex. Thus the difficulty might be removed by per-
forming a coupled-channel analysis of both the
elastic and inelastic beams.

V. LOSS PROFILES: Al(111) AND Al(100)

The most important feature of the loss profiles
disclosed by our analyses is their kinematical
character. As the incident energy and all of the
angular beam parameters are held fixed, the
elastic-scattering vertex in the D-L contribution
to the loss profile is rigorously constant. The
elastic vertices in the L-D and D-L-D contribu-
tions depend on the variable $E-w$, and hence vary
as w is changed to generate the loss profile. In
general, however, the range, $\Delta w \sim 10$ eV, over which
w is varied is small relative to the energy scale
of fine structure in the energy profile. There-
fore, near a prominent peak in the elastic energy
profile this vertex also exhibits roughly "kinemat-
ic" behavior in that to within a constant scale fac-
tor it behaves as if the prominent peak were ap-
proximately a kinematical primary Bragg peak.

We illustrate this result for the Al(111) example
analyzed by Bagchi and Duke[9] in Fig. 8. As seen
in Fig. 8(b) the incident-beam energies 40, 50,
and 60 eV span a Bragg peak in the kinematical
energy profile (dashed line). The corresponding
dynamical energy profile (solid line) also exhibits
a maximum near this energy. Figure 8(a) indi-
cates that for some values of w the loss profiles
are quite sensitive to the primary-beam energy
(especially near the bulk-plasmon loss energy)
but not to the distinction between the dynamical
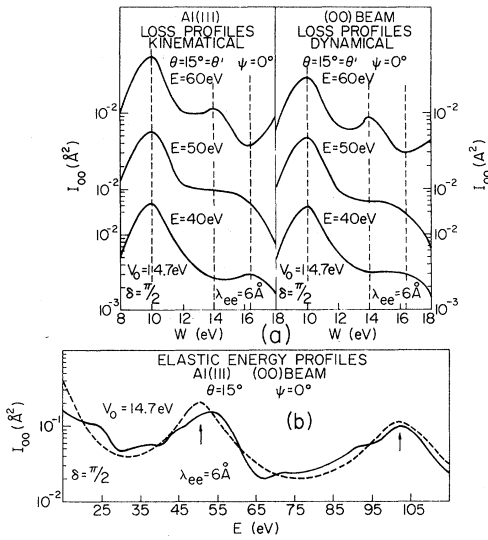and kinematical model. In particular, the energy

FIG. 8. (a) The kinematical and dynamical loss profiles for electrons diffracted in the (00) beam from Al(111). The profiles are shown for various energies above and below the kinematical bragg energy ($E_B = 50$ eV) in the elastic energy profile of the (00) beam. The plasmon-dispersion relations used in constructing the figure are those used by Bagchi and Duke (Ref. 9) and indicated in the caption to Fig. 2. The parameters used in describing the elastic electron-solid scattering are indicated in the figure. Vertical dashed lines are included for convenience in visualization. (b) A plot of the kinematical (dashed line) and dynamical (solid line) elastic intensity profiles obtained using these parameters [see also Bagchi and Duke (Ref. 9)]. Arrows indicate the kinematical primary Bragg energies. All beam parameters are noted in the figure.

of the surface-plasmon peak remains constant in both the kinematical and dynamical models even when the incident-beam energy is varied.

In order to verify that the correspondence between the kinematical and dynamical loss profiles is not an accidental consequence of the parameters used in Bagchi and Duke's analysis of Al(111), we also examined these profiles for Al(100) using parameters to describe the elastic scattering which are known to lead to substantial dynamical effects in the energy profiles (Figs. 1–3). A typical elastic and inelastic rotation diagram at the incident-beam energy ($E = 29$ eV) characteristic of some secondary structure in the elastic energy profile is shown in Fig. 9. Both strong dynamical effects and pronounced consequences of the coherence between the D-L and L-D energy-loss processes are evident in the figure. The loss profiles associated with these distinct regions of the rotation diagram (i.e., $\psi = 5°$, $\psi = 15°$, and $\psi = 40°$) are shown in Fig. 10. The close correspondence between the kinematical and dynamical profiles is obvious from the figure. In particular, the values

of w at which the peaks occur are determined by the plasmon spectral densities $\mathrm{Im}D(\vec{p}, w)$ rather than by the behavior of the elastic vertex functions appearing in the expressions for the cross sections. Thus, an analysis of the loss profiles based on the kinematical two-step diffraction model does suffice to determine the consequences of surface plasmon dispersion, even though this model does not suffice to describe inelastic energy profiles and rotation diagrams.

VI. SUMMARY AND CONCLUSIONS

In this and the preceding[1] paper we examined the dynamical (i.e., multiple-scattering) effects on the predictions for the ILEED intensities obtained by using Duke and Laramore's quantum field theory of inelastic diffraction.[2] We formulated this
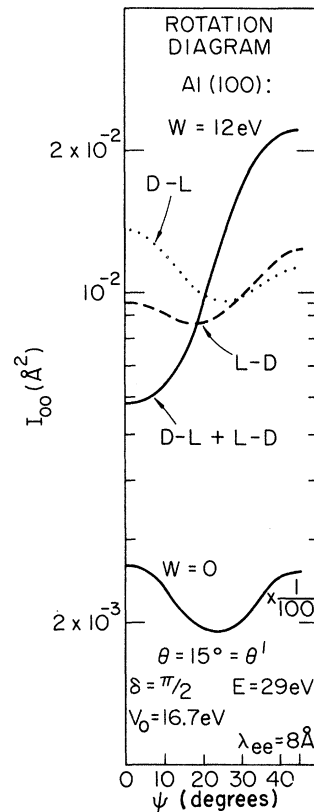

FIG. 9. Elastic ($w = 0$) and inelastic ($w = 12$ eV) rotation diagrams of the (00) beam of electrons, incident at $E = 29$ eV, scattered from Al(100). In a kinematical model, all of the curves shown in the figure would be horizontal straight lines. The dashed curve gives the loss-before-diffraction contribution to the $w = 12$ eV inelastic cross sections whereas the dotted curve gives the diffraction-before-loss contribution to them. The plasmon-dispersion relations used in constructing this figure are specified in the caption to Fig. 2. The beam parameters and elastic-scattering parameters used in the calculation are noted in the figure.
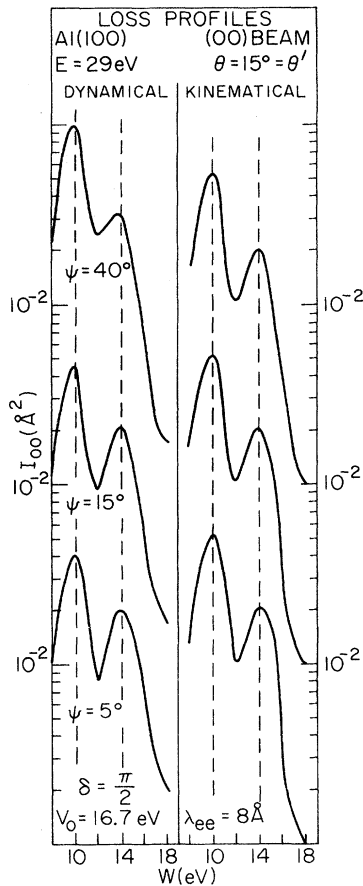
LOSS PROFILES
Al(100)   (OO)BEAM
E = 29eV $\theta = 15° = \theta'$
DYNAMICAL | KINEMATICAL

$\psi = 40°$

10^{-2} 10^{-2}

10^{-2} 10^{-2}

$\psi = 15°$

10^{-2} 10^{-2}

$\psi = 5°$

$\delta = \dfrac{\pi}{2}$

$V_0 = 16.7$ eV $\lambda_{ee} = 8$ Å

10   14   18   10   14   18
W(eV)

FIG. 10. Dynamical (left-hand panel) and kinematical
(right-hand panel) loss profiles for the (00) beam of elec-
trons, incident at $E = 29$ eV, scattered from Al(100). The
loss profiles shown are associated with these azimuthal
angles for which the rotation diagram in Fig. 9 predicts
quite different values of the intensity at a loss energy (w)
of 12 eV. The elastic-scattering and beam parameters,
identical to those used constructing in Fig. 9, are indi-
cated in the figure. The plasmon parameters, also identi-
cal to those used for Fig. 9, are specified in the caption
of Fig. 2. The kinematical nature of the loss profiles
despite the dynamical nature of the rotation diagrams is
evident upon examining the results shown in Figs. 9 and
10.

dynamical theory of ILEED from solid surfaces by
extending the previously developed[3] two-step model
of ILEED in two major ways. (a) The incident
electron is permitted to scatter elastically from
the lattice ion-cores potential an arbitrary number
of times both "before" and "after" an inelastic loss
event. These events result in a renormalization
of the elastic vertex in the two-step mechanism as
described in the preceding paper. (b) The inci-
dent electron also is permitted to scatter elastical-
ly both before and after the loss event. We refer
to the sum of all such scatterings as a three-step
process which describes renormalized diffraction

before and after loss.

Following our derivation in the preceding paper
of the analytical formulas for the cross sections,
we presented herein sample calculations of ILEED
intensities from Al(100) and Al(111) in order to
illustrate the dynamical structures which occur, to
identify their origin, and to estimate their impor-
tance in achieving an interpretation of the inelastic
intensities. In particular, we examined in detail
the conditions under which the kinematical two-
step diffraction model[3,9-11] can be used to deter-
mine plasmon-dispersion relations. This examina-
tion led to the important conclusion that surface-
plasmon dispersion and damping can be extracted
from experimental loss (and possibly angular) pro-
files by use of the kinematical two-step analysis.
Bulk-plasmon dispersion can be extracted only
from loss profiles, if at all. We made no attempt
to determine bulk-plasmon dispersion and damping,
preferring to use the dispersion relation already
obtained experimentally by high-energy $(E \sim 10^4$ eV)
electron-transmission experiments from thin
films.[9]

During our study of multiple-elastic-scattering
effects, we discovered that the magnitude and
prominence of their manifestations depend sensi-
tively on the mode of presentation selected to dis-
play the inelastic diffraction intensities. They are
most prominent for those presentations in which
the energy or angular variables of the renormalized
elastic-scattering vertices span a wide range (e.g.,
energy profiles or inelastic rotation diagrams).
Of special interest to us in this regard was the de-
termination of whether the consequences of dynam-
ical elastic diffraction could be distinguished from
those of (kinematical) momentum conservation
during the electron's excitation of bulk-loss modes
(i.e., sideband diffraction[7]). Our examination of
both the energy and angular profiles led to the con-
clusion that such a distinction could be made only
if the model parameters were known a priori. It
cannot be made on the basis of qualitative features
of the data like a four-peaked structure in the in-
elastic energy associated with a single peak in the
elastic energy profile. Therefore, we conclude
that it is not possible to use in any simple way the
kinematic momentum-conservation laws for bulk
excitations of the solid to extract from experi-
mental ILEED data the dispersion relations of these
excitations.

Turning to a final conclusion of a more technical
nature, we discovered that our isotropic-scatterer
model predicts that the contributions to the ILEED
intensities of the D-L-D three-step process usually
are quite small compared to those from the two
other (renormalized) D-L and L-D processes.
Consequently, all of our predicted manifestations
of dynamical effects are associated with the re-

normalization of the elastic vertices in the two-step mechanism. Our results also indicate that the surface contribution to the inelastic-scattering cross sections may be large and exhibit dynamical structure for loss energies (w) close to the bulk-plasmon threshold (see e.g., Fig. 5). Consequently, the surface contribution to the predicted dynamical effects may be dominant for a certain range of incident-beam energies even for values of w at which bulk-plasmon loss processes generally dominate the cross sections.

Surveying our results, we argue that our analysis of dynamical elastic-scattering effects in ILEED intensities has been successful in establishing our main objective: The conclusion that these dynamical effects are irrelevant for extracting surface-plasmon-disperion relations from experimental data *provided one selects the proper subset of data (i.e., loss profiles) to analyze.* Our description of observed dynamical effects[9-11,18,19] has been less successful. On the one hand we did establish that much of the observed[19] fine structure in large-w inelastic energy profiles could be caused by dynamical elastic-scattering effects as anticipated earl-

ier.[9] However, the persistent failure of the experimental measurements[9,11,18] to exhibit the large-angle peak of the surface-plasmon "doublet" in the angular profile, except near the energies of maxima in the elastic energy profile, is not explained either by our analysis, or by a kinematical two-step analysis using a realistic elastic electron-ion-core scattering amplitude.[17] As such a suppression of the large-angle peak is characteristic of the L-D processes, we think that this failure of our analysis probably reflects a failure of low-order perturbation theory in the inelastic vertex because a more extensive coupled-channel analysis would indicate a prominent role of the D-L process only near maxima in the elastic scattering cross sections.

[1]C. B. Duke and U. Landman, preceding paper, Phys. Rev. B **6**, 2956 (1972).
[2]C. B. Duke and G. E. Laramore, Phys. Rev. B **3**, 3183 (1971).
[3]G. E. Laramore and C. B. Duke, Phys. Rev. B **3**, 3198 (1971).
[4]C. W. Tucker, Jr. and C. B. Duke, Surface Sci. **24**, 31 (1971).
[5]C. B. Duke, G. E. Laramore, B. W. Holland, and A. M. Gibbons, Surface Sci. **27**, 523 (1971).
[6]C. W. Tucker, Jr. and C. B. Duke, Surface Sci. **29**, 237 (1972).
[7]C. B. Duke, G. E. Laramore, and V. Metze, Solid State Commun. **8**, 1189 (1970).

[8]C. B. Duke, A. J. Howsmon, and G. E. Laramore, J. Vac. Sci. Technol. **8**, 10 (1971).
[9]A. Bagchi and C. B. Duke, Phys. Rev. B **5**, 2784 (1972).
[10]C. B. Duke and A. Bagchi, J. Vac. Sci. Technol. **9**, 738 (1972).
[11]A. Bagchi, C. B. Duke, P. J. Feibelman, and J. O. Porteus, Phys. Rev. Letters **27**, 998 (1971).
[12]G. E. Laramore and C. B. Duke, Phys. Rev. B **5**, 267 (1972).
[13]C. B. Duke, and C. W. Tucker, Jr., Phys. Rev. B **3**, 3561 (1971).
[14]P. J. Feibelman, C. B. Duke, and A. Bagchi, Phys. Rev. B **5**, 2436 (1972).
[15]C. B. Duke and C. W. Tucker, Jr., Surface Sci. **15**, 751 (1969).
[16]C. B. Duke, J. R. Anderson, and C. W. Tucker, Jr., Surface Sci. **19**, 117 (1970).
[17]C. B. Duke and U. Landman, Bull. Am. Phys. Soc. **17**, 600 (1972); C. B. Duke, U. Landman, and J. O. Porteus, J. Vac. Sci. Technol. (to be published).
[18]J. O. Porteus (unpublished); J. O. Porteus and W. N. Faith, J. Vac. Sci. Technol. **9**, 1062 (1972).
[19]J. M. Burkstrand and F. M. Propst, J. Vac. Sci. Technol. **9**, 731 (1972).